

Experimental Investigation on Penetration of Rotating Magnetic Perturbations into the Tokamak Plasma

M. Kobayashi¹, T. Tuda², K. Zhai¹, H. Kojima¹, K. Tashiro¹, S. Takamura¹

¹Department of Energy Engineering and Science, Graduate School of Engineering, Nagoya University, Nagoya 464-8603, Japan

²Department of Fusion Plasma Research, Naka Fusion Research Establishment Japan Atomic Energy Research Institute, Naka 311-0193, Japan

1. Introduction

The penetration process of perturbation field into the rotating tokamak plasma is one of the most important physics in terms of the global stability because the resonant magnetic perturbation might drive the uncontrollable MHD mode if it penetrates deep into the plasma, and finally lead to a major disruption. In order to prevent such a catastrophe, the structure and intensity of perturbation field of DED (dynamic ergodic divertor) [1,2] have been carefully adjusted by taking account of the mode mixing and the skin type penetration [2]. But there seems to be no clear criterion of those adjustments.

In the present work we investigated the penetration process of the externally applied magnetic field into the tokamak plasma in terms of the mode structure, by employing a small magnetic probe inserted into the plasma in the small research tokamak device CSTN-IV [3] powered by IGBT inverter power supply for a poloidally Rotating Helical Field (RHF). We also performed the numerical calculations by solving the resistive MHD reduced set of equations and compare it with the experimental results to discuss the behavior of magnetic field in the plasma.

2. Description of Experiments and Numerical Simulations

CSTN-IV has the major radius of 0.4 m and the minor radius of 0.1 m. A toroidal magnetic field is kept at around 0.086 T in steady state. The electron temperature and density are about 10 eV and $1.5 \times 10^{18} \text{ m}^{-3}$ respectively, which were measured with a triple probe at $r = 5 \text{ cm}$. RHF of 10

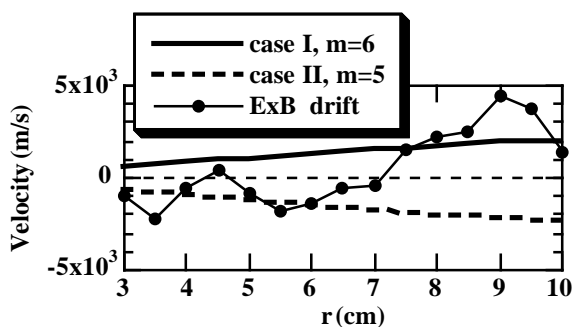


Fig. 1 Radial profiles of phase velocity of perturbation with $m = 5$ and 6 at 20kHz , comparing with $E \times B$ drift calculated from T_e and floating potential measured with a triple probe.

ms pulse was applied during the tokamak discharge of 15 ms pulse. The RHF is induced with two sets of local helical coils (LHC) which are installed outside the vacuum vessel at eight toroidal sections among 16 with poloidal and toroidal mode number $(m, n) = (6, 1)$ [1]. These coils are energized independently by the IGBT inverter power supply with rectangular AC voltage of 90 degrees phase difference between these two coils to produce the traveling

perturbation. The radial and poloidal components of perturbation field on an equatorial plane were measured with small magnetic probes. A resonance surface to the perturbation of $m/n = 6/1$ was estimated to be located at around $r = 7.5$ cm from the q profile, which is calculated from the measured poloidal field taking a toroidal effect into account. At the resonance surface the amplitude of perturbation field is about 1 Gauss which gives $w = 4(rqB_r/mqB)^{1/2} \sim 3$ cm as a saturated island width, while the poloidal field of plasma current is about 20 Gauss. From those experimental values, the resistive MHD parameters are estimated as follows: The resistive diffusion time $\tau_R = \mu_0 a^2 / \eta \sim 350 \mu\text{s}$, where a is the plasma radius and the plasma resistivity $\eta \sim 1.2 \times 10^{-3} T_e^{-3/2}$ (m). Alfvén transit time $\tau_A = R_0 q / V_A \sim 2.5 \mu\text{s}$, where $V_A = B_z / \sqrt{\mu_0} \sim 1.6 \times 10^6$ m/s is the typical Alfvén speed. These values give us the relatively small magnetic Reynolds number $S = \tau_R / \tau_A \sim 140$. The rotating direction of perturbation field can be controlled by changing the relative phase between A and B coil currents. In this paper henceforth “case I” means the case with the perturbation rotating in the same direction as that of ion diamagnetic drift, while “case II” the perturbation rotating in electron diamagnetic drift direction. Both cases were studied in the present experiments.

We also performed numerical simulations by solving the resistive MHD reduced set of equations of a low cylindrical plasma with the transport equation of electron temperature [4]. In the simulation the pure $m/n = 6/1$ mode perturbation field was applied to the plasma as an RHF and the resistive MHD parameters were set to the values obtained above. Since the model does not include any intrinsic plasma rotation, we changed the frequency of perturbation from 5kHz to 40kHz taking into account the $\mathbf{E} \times \mathbf{B}$ drift (i.e. plasma inertia [5]) which is shown in Fig. 1 together with the poloidal phase velocity of perturbations. The result of 5kHz is considered to correspond to the case I while 40kHz to the case II.

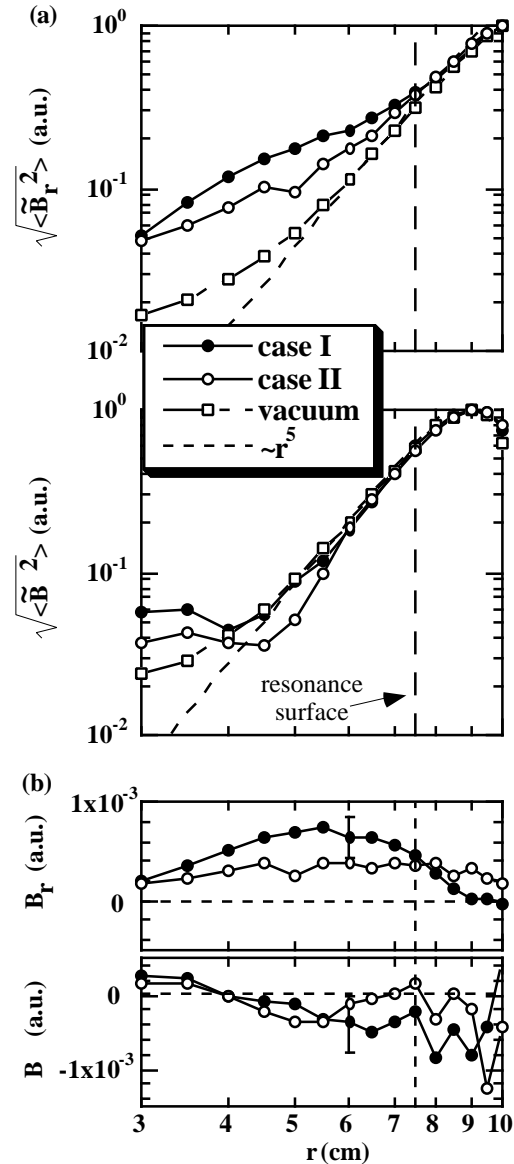


Fig. 2 (a) Radial distributions of oscillating B_r and B in the cases of I and II. The square root of peak value of 20kHz in the power spectra at each radial position is plotted. (b) Differentials in the oscillating field between the cases with and without plasma.

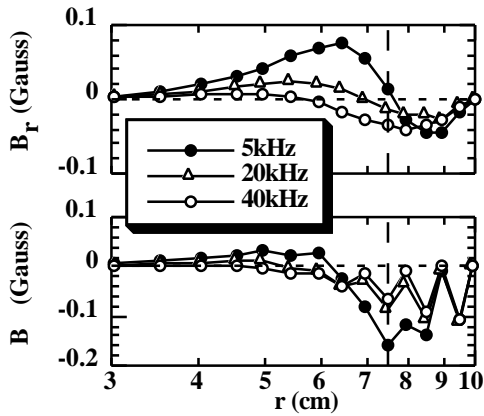


Fig. 3 Radial distributions of differentials in oscillating field between the cases with and without plasma, which are obtained from the simulation. A vacuum field is assumed to be proportional to r^5 .

3. Results and Discussion

Figure 2 (a) shows the experimental results of radial distributions of perturbation field \tilde{B}_r and \tilde{B} with and without plasma in the case of 20kHz RHF. We see that the vacuum fields decrease along r^5 lines as going to the inside of chamber, according to a multi-polar approximation r^{m-1} . Figure 2 (b) shows the plasma response corresponding to difference between the values with and without tokamak plasma. It should be noted that the radial component of perturbation is amplified in the plasma almost over the whole radial positions, and that its amplification become large in the case I inside the resonance surface. On the other hand,

the poloidal perturbation field was observed to be attenuated in the plasma with respect to the value in vacuum at around the resonance surface in both cases of I and II, but at $r < 4$ cm it is amplified. Figure 3 shows the differentials in perturbation field between the cases with and without plasma obtained by the simulations in a good agreement with the experiments. That is, an amplification of the radial magnetic field, an attenuation near the resonance surface and an amplification deep inside the plasma of poloidal field are all reproduced in the simulation.

These modifications of the external perturbation in Fig. 2 (b) and 3 are clearly explained in Fig. 4 which shows the instantaneous picture of (a) the helical flux contour and (b) the perturbed current profile in two dimensional space of radius and poloidal angle, where the magnetic island is formed with the width of about 1.5 cm and is still observed to appear at the case with 40kHz. In this figure the redistribution of toroidal plasma current is observed, which comes from the formation of magnetic islands. Such the current redistribution gives rise to the amplification of \tilde{B}_r at $r < r_s$, and the attenuation of \tilde{B}_r at $r > r_s$. It also attenuates the \tilde{B} at around the resonance surface while amplifies deep inside the plasma. Obviously as the perturbation frequency increases the shielding effect becomes dominant. That is the reason why in the case II (40kHz) the modification become small compared with the case I (5kHz) and the attenuation of \tilde{B}_r at around the resonance surface due to shielding current becomes clear.

The attenuation of \tilde{B}_r observed in simulation at $r > r_s$ does not occur in the experiments. It is considered due to the ergodization of flux surfaces which comes from the overlapping of sidebands at $r > r_s$ [1]. Since the enhanced transport in the ergodic region tends to prevent any peaked current distribution, the amount of attenuation due to the perturbed current at $r > r_s$ would become small compared to that of amplification which comes from the perturbed current at $r < r_s$. It would result in the amplification of \tilde{B}_r at $r > r_s$ rather than the attenuation.

It is also observed that the region with the main attenuation of \tilde{B} shifts from $r = 7.5$ cm to 5

cm in the case II. This is expected by a substantial growth of $m = 5$ islands because as shown in Fig. 1 the phase velocity of $m = 5$ in the case II becomes almost equal to that of $\mathbf{E} \times \mathbf{B}$ drift at $r = 6$ cm where the islands of $m = 5$ appear in Poincaré plot of field tracing.

From the above discussion, it can be said that when considering the penetration process of magnetic perturbation into the tokamak plasma and in order to have the stable DED operation, we should take into account the mode structure of perturbation field and the radial profile of the intrinsic plasma rotation at the same time.

4. Conclusion

A penetration process of magnetic perturbation into the tokamak plasma was investigated with measuring the magnetic field inside the plasma. It was found that in the case where magnetic islands were formed the radial component of perturbation field was amplified in plasma due to the current redistribution coming from the deformation of flux surface. The poloidal component of perturbation field is also amplified deep inside the resonance surface. The modification also takes place at the sideband resonance, which means that the sidebands have a substantial effect on the penetration process. Therefore it is necessary to take into account not only the frequency of the RHF but also its direction, mode structure and the radial profile of the intrinsic plasma rotation at the same time when considering the penetration process of magnetic perturbation into the tokamak plasma in the DED operation.

Acknowledgments

Authors would like to thank Drs. A. W. Morris, T. C. Hender, R. J. Buttery, K. H. Finken, Y. Uesugi and N. Ohno for their fruitful discussions and Mr. M. Takagi for his technical assistance. The present work is supported financially by Grant-in-Aid for Scientific Research (A) No. 09308018 of The Ministry of Education, Science, Sports and Culture.

References

- [1] TAKAMURA, S., YAMADA, H., OKUDA, T., Nucl. Fusion **28** (1988) 183.
- [2] FINKEN, K. H., EICH, T., ABDULLAEV, S. S., et al., J. Nucl. Mater. **266-269** (1999) 495.
- [3] TAKAMURA, S., HAYASHI, K., TASHIRO, K., J. Plasma and Fusion Res. **74** (1998) 38.
- [4] KURITA, G., TUDA, T., AZUMI, M., TAKIZUKA, T., TAKEDA, T., Nucl. Fusion **34** (1994) 1497.
- [5] FITZPATRICK, R., HENDER, T. C., Phys. Fluids **B3** (1991) 644.

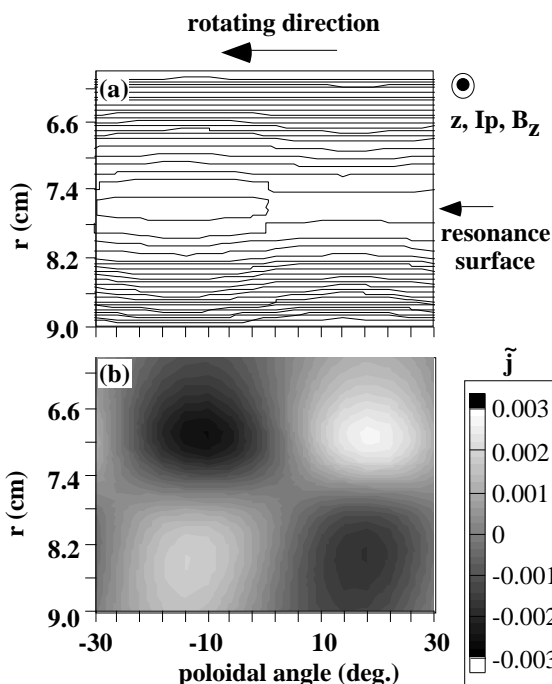


Fig. 4 (a) Contours of helical flux function at around the resonance surface and (b) 2-D profile of the perturbed current density which is normalized by $B_z/(\mu_0 a)$, where a is a minor radius and B_z a toroidal field, in the case of 5kHz. Perturbed current is $\sim 3\%$ of equilibrium plasma current.